

# Low-Cost, Open-Source Colorimetric Platform for Point-of-Care (POC) anti-Human Papillomavirus Type 16 (HPV16) Antibody Detection

Joshua Eger<sup>1,3</sup>, Akshansh Kaushik<sup>2</sup>, Tej Patel<sup>2</sup>, Karen S. Anderson<sup>2</sup>, Jennifer Blain Christen<sup>3</sup>

**Abstract**—Human papillomavirus (HPV) is a leading cause of anogenital and head and neck cancers. HPV type 16 (HPV16) is a significant high-risk strain due to its strong association with these malignancies. The burden of HPV-related cancers is particularly severe in low and middle-income countries (LMICs), where access to diagnostic tools is limited. This work introduces a low-cost, point-of-care (POC) colorimetric platform for detection of antibodies against HPV16. The lateral flow immunoassay (LFIA) developed uses immobilized HPV16 CE2 and E7 proteins for antibody capture and colloidal gold-conjugated secondary for colorimetric labeling. Quantitative readout is achieved via an imaging device that incorporates open-source electronics and 3D-printed components. Analytical sensitivity experiments determined a limit of detection (LOD) at 46 ng/mL. Clinical evaluation of plasma samples ( $n = 20$ ) from head and neck cancer patients ( $n = 15$ ) and healthy individuals ( $n = 5$ ) yielded 94.7% sensitivity, 90.5% specificity, and 92.5% overall accuracy. This study identified a moderate-to-high prevalence of anti-HPV16 antibodies in head and neck cancer patients, with 66.7% testing positive. These results suggest that our platform is a viable tool for detection of anti-HPV16 antibodies, particularly in resource-limited settings where cost-effectiveness and accessibility are crucial.

**Clinical relevance**— The reported approach enables screening for HPV-driven oropharyngeal and anogenital cancer from a finger stick.

## I. INTRODUCTION

Human papillomavirus (HPV) is a prevalent sexually transmitted infection with over 100 different strains [1]. HPV type 16 (HPV16) is characterized as a significantly high-risk strain due to its strong association with anogenital and head and neck cancers [2]. The burden of HPV-related cancers is especially pronounced in low and middle-income countries (LMICs). Access to effective screening and treatment is often limited in LMICs, leading to disproportionately higher incidence and mortality rates [3]. Persistent HPV16 infection can result in the development of precancerous lesions that can progress to invasive cancer [4]. Detection of HPV16 infection is crucial for effective intervention and cancer prevention, especially in resource-constrained settings.

Point-of-care (POC) approaches utilizing smartphones for colorimetric analysis provide an innovative solution for antibody detection [5]. These methods can be accessible, leveraging the ubiquity of smartphones to facilitate rapid and accurate antibody detection on-site. However, using

smartphones in POC applications also presents challenges. Smartphones are often more expensive than low-cost camera modules, image quality and camera capabilities vary widely between devices, and regular operating system updates are required for maintaining functionality [6]. Despite these challenges, POC technologies present significant potential for improving antibody detection, especially in LMICs where access to traditional laboratory facilities may be limited.

In this work, we present a POC anti-HPV16 antibody detection platform consisting of a lateral flow immunoassay (LFIA) and colorimetric detection instrument. The LFIA targets anti-HPV16 antibodies and uses colloidal gold nanoparticle-conjugated secondary for labeling. The colorimetric reader enables quantitative analysis of LFIAs using low-cost, open-source hardware and software. This platform aims to provide accessible and reliable diagnostics for improved detection of HPV16 at the POC.

## II. MATERIALS AND METHODS

### A. LFIA Test Strip and Cartridge Assembly

In this work, we developed a multiplexed, indirect LFIA for anti-HPV16 antibody detection (Fig. 1a). The C-terminal fragment of HPV16 E2 (CE2) and HPV16 E7 were used for antibody capture. These proteins were printed onto adhesive-backed nitrocellulose membrane (Sartorius, Göttingen, Germany) using an automated dispensing system (BioDot, Irvine, CA). CE2 ( $0.5 \mu\text{L} \times 0.3 \text{ mg/mL}$ , GenScript, Piscataway, NJ) and E7 ( $0.5 \mu\text{L} \times 0.4 \text{ mg/mL}$ , GenScript, Piscataway, NJ) were printed at the test lines. Human immunoglobulin G (IgG) ( $0.5 \mu\text{L} \times 0.5 \text{ mg/mL}$ , Jackson ImmunoResearch Labs, West Grove, PA) was printed at the positive control line. One site was left blank for background measurements. A separation membrane (Cytiva, Marlborough, MA) and sample pad (C083, MilliporeSigma, Burlington, MA) were stacked at the proximal end of the nitrocellulose membrane; two absorbent pads (CF7, Whatman, Cytiva, Marlborough, MA) were stacked at the distal end. The assembly was cut into individual test strips using a guillotine cutting module (Kinematic Matrix 2360, Ascential Technologies, San Diego, CA). Individual test strips were then enclosed using 3D-printed acrylonitrile butadiene styrene (ABS) cartridges. The top component contains fluid delivery ports and a visualization window (Fig. 1c). The bottom component contains guides to constrain the strip in the correct position (Fig. 1b). The cartridge assembly measures  $78.0 \text{ mm} \times 22.0 \text{ mm} \times 7.2 \text{ mm}$ .

<sup>1,3</sup>J. Eger is with the School of Biological and Health Systems Engineering. <sup>2</sup>A. Kaushik, T. Patel, and K. Anderson are with the Center for Personalized Diagnostics, Biodesign Institute. <sup>3</sup>J. Eger and J. Blain Christen are with the Center for Bioelectronics and Biosensors, Biodesign Institute, Arizona State University, Tempe, AZ 85281, USA. Corresponding author e-mail: Jennifer.BlainChristen@asu.edu.

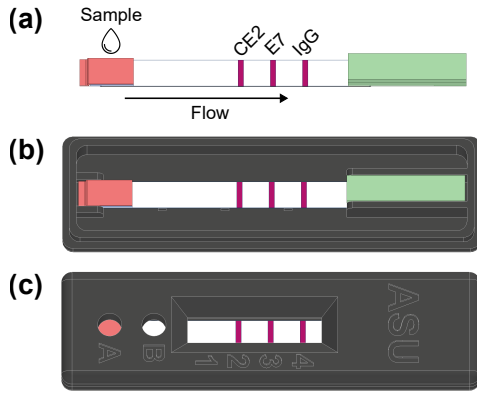


Fig. 1. (a) LFIA test strip schematic with nitrocellulose (white), adhesive backing (grey), sample pad (blue), separation membrane (red), and absorbent pads (green) indicated. (b) LFIA test strip positioned in the bottom component of the 3D-printed cartridge. (c) LFIA test strip fully enclosed by the addition of the top component.

### B. Dilution Series and Patient Sample Preparation

A dilution series was prepared and patient plasma samples ( $n = 20$ ) were collected to assess analytical sensitivity and clinical efficacy, respectively. The dilution series was prepared by first diluting mouse anti-HPV16 E7 monoclonal antibodies (1 mg/mL, Bio-Rad Laboratories, Hercules, CA) in phosphate-buffered saline with 0.2% Tween 20 (PBST) (Sigma-Aldrich, St. Louis, MO) to a concentration of 33  $\mu\text{g/mL}$  (1:30 dilution). Subsequent solutions were produced via 2-fold serial dilution, resulting in concentrations from 17  $\mu\text{g/mL}$  (1:60 dilution) to 33 ng/mL (1:30720 dilution). Samples from head and neck cancer patients ( $n = 15$ ) and healthy individuals ( $n = 5$ ) were commercially sourced from Indivumed Therapeutics (Hamburg, Germany). Patient samples were diluted to a 1:30 ratio by adding 1  $\mu\text{L}$  of plasma to 29  $\mu\text{L}$  of PBST, yielding a final volume of 30  $\mu\text{L}$  per sample. Colloidal gold nanoparticles (40 nm, OD 10, DCN Dx, Carlsbad, CA) were conjugated to protein G (0.012 mg/mL, GenScript, Piscataway, NJ) for colorimetric signal generation.

### C. Colorimetric Detection Platform

The colorimetric detection platform (Fig. 2) was designed with an emphasis on utilizing low-cost, open-source components (Table I) to ensure accessibility and ease of replication. The housing and structural components were fabricated in ABS using an FDM 3D printer (MK3S+, Prusa Research, Prague, Czech Republic). The 3D-printed components are engineered for easy assembly; the modular design allows for alternative fabrication methods like laser cutting to assemble the reader on-site, providing flexibility in resource-constrained settings. Diffuse LED backlights (Adafruit Industries, New York, NY) were incorporated for consistent and uniform illumination of the LFIA test strips (Fig. 2a, c, d). A 5 megapixel (MP) serial peripheral interface (SPI) camera module (Arducam, Japan) was used to capture images (Fig. 2a, c). A microcontroller (Mega 2560 Rev3, Arduino, Somerville, MA) was used for integrating the

electrical components and managing operation of the device (Fig. 2b). An open-source hardware interface tool (Mega, Arducam, Japan) was employed to retrieve images from the device and adjust parameters such as brightness, contrast, saturation, exposure, color balance, and focus. An open-source image analysis software (ImageJ, National Institutes of Health, Bethesda, MD) was used to measure colorimetric signal intensities at the test/control lines.

TABLE I  
COLORIMETRIC DETECTION INSTRUMENT BILL OF MATERIALS

Component	Quantity	Unit Cost	Total Cost
Microcontroller	1	\$41.14	\$41.14
Camera Module	1	\$34.99	\$34.99
LED	2	\$1.95	\$3.90
ABS	0.092	\$32.99	\$3.02
<b>Total</b>			<b>\$83.05</b>

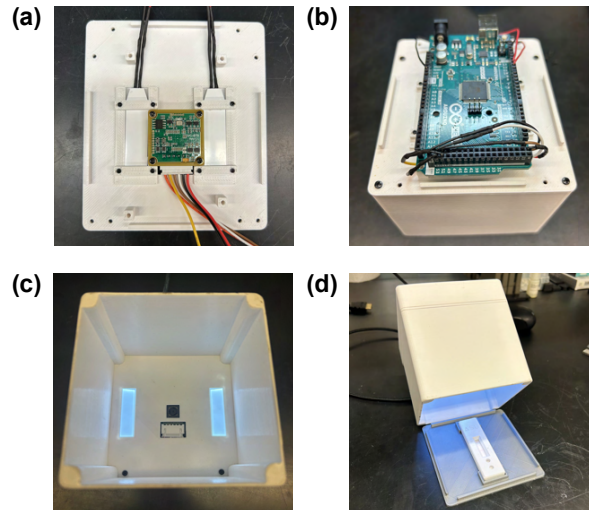


Fig. 2. Top view of the colorimetric detection instrument showing the (a) LEDs, camera module and (b) microcontroller. (c) Internal view of the reader enclosure with the LEDs and camera module shown. (d) Reader open showing illumination of an LFIA cartridge.

## III. RESULTS AND DISCUSSION

### A. Analytical Sensitivity

Analytical sensitivity of the LFIA colorimetric detection platform for anti-HPV16 antibody detection was assessed by determining the limit of detection (LOD). The LOD represents the lowest antibody concentration that can be reliably detected and the point at which the analyte signal is distinguishable from the instrument/method noise [7]. The LOD was established by analyzing a dilution series of known monoclonal antibody concentrations against HPV16 E7 (Fig. 3a). By determining the LOD, we aimed to evaluate the system's sensitivity and ability to detect low antibody concentrations, which are indicative of early-stage and/or past infection [8].

Analytical methods based on measurements of blank samples are effective for determining LOD when the analyte is not in solution [9]. The LOD y-intercept ( $y_{LOD}$ ) was determined using the equation  $y_{LOD} = \mu_{blank} + 3.3\sigma_{blank}$ , where  $\mu_{blank}$  and  $\sigma_{blank}$  are the mean signal intensity and standard deviation of the blank samples, respectively [9], [10]. In order to calculate the concentration (LOD) at which the signal intensity is equal to  $y_{LOD}$ , we employed a modified four-parameter logistic (4PL) regression model given by the general equation

$$f(x) = d + \frac{a - d}{1 + \left[\frac{\log(x)}{c}\right]^b}, \quad (1)$$

where  $a$  is the maximum asymptote,  $b$  is the scale factor (Hill's slope),  $c$  is the inflection point and  $d$  is the minimum asymptote [11]. LOD was calculated by rearranging Eq. 1 and substituting  $y_{LOD}$  for  $f(x)$  and  $LOD$  for  $x$ , yielding the equation

$$LOD = 10^{c \left( \frac{a-d}{y_{LOD}-d} - 1 \right)^{\frac{1}{b}}}. \quad (2)$$

The results showed a clear correlation between antibody concentration and color intensity on the LFIA test strips. The lowest visibly detectable concentration was 65 ng/mL (Fig. 3a). Below this concentration, the color intensity was indistinguishable from the negative control. The 4PL regression model generated to fit the data was  $f(x) = 1.137 - 1.139/[1 + \log(x)/3.208]^{6.13}$  with  $R^2 = 0.9931$ ; the LOD is 46 ng/mL (Fig. 3b). These results were compared to gold standard, benchtop approaches in addition to similar low-cost, POC methods. Inan et. al. report a LOD for anti-HPV16 E7 antibody detection of 2.87 ng/mL using an enzyme-linked immunosorbent assays (ELISA) [12]. The method demonstrated superior analytical sensitivity, but it involved greater complexity and required expensive instrumentation for quantification. Parra et. al. demonstrate a detection limit on the order of 1  $\mu$ g/mL using a low-cost, POC system [13]. The approach yielded decreased analytical sensitivity at a higher cost (\$1,226) compared to the platform presented in this work. The results suggest that our colorimetric detection platform offers competitive analytical sensitivity while maintaining the advantages of simplicity and cost-effectiveness.

### B. Clinical Evaluation

Patient plasma samples were evaluated to assess the clinical efficacy of our system for anti-HPV16 antibody detection. Clinical performance was determined using several key metrics: sensitivity, specificity, positive predictive value (PPV), negative predictive value (NPV), and accuracy. Sensitivity is the true positive (TP) rate and reflects the test's ability to correctly identify the presence of target antibodies. Specificity is the true negative (TN) rate and indicates the test's ability to correctly identify absence of target antibodies [14]. PPV is the probability that subjects with a positive screening result truly have target antibodies, whereas NPV is the probability that subjects with a negative screening result

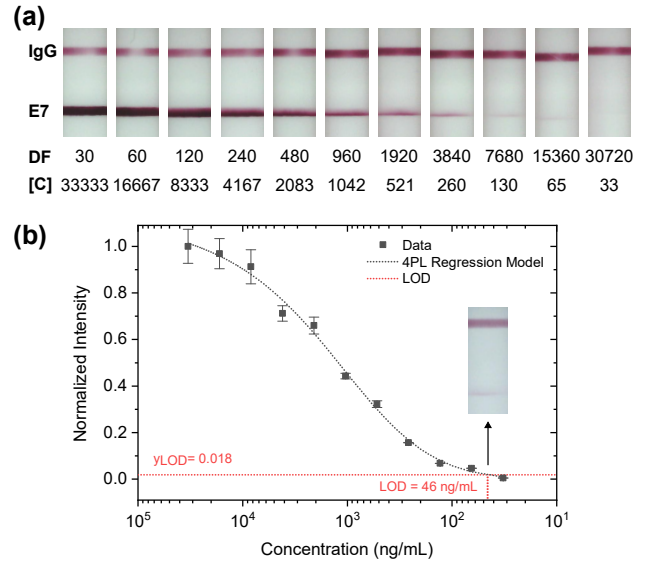


Fig. 3. (a) Dilution series with corresponding dilution factor (DF) and concentration (C) in ng/mL listed. (b) Analytical sensitivity with 4PL regression model plotted and LOD indicated.

truly do not have target antibodies [15]. Accuracy reflects the test's overall ability to correctly classify both positive and negative samples [16].

We analyzed plasma samples ( $n = 20$ ) from head and neck cancer patients ( $n = 15$ ) and healthy individuals ( $n = 5$ ) using our colorimetric detection platform (Fig. 4a). Images of the CE2, E7, and IgG sites were acquired and subsequently processed for signal intensity quantification. Performance metrics were calculated according to standard equations [17]–[19]:

$$Sensitivity = TP/(TP + FN) \quad (3)$$

$$Specificity = TN/(FP + TN) \quad (4)$$

$$PPV = TP/(TP + FP) \quad (5)$$

$$NPV = TN/(TN + FN) \quad (6)$$

$$Accuracy = \frac{TP + TN}{TP + TN + FP + FN} \quad (7)$$

The results demonstrated mean signal-to-background ratios (SBR) of 6.0:1 and 3.5:1 for positive CE2 and E7 tests, respectively (Fig. 4b). Mean IgG SBR for negative and positive test results were 5.6:1 and 5.0:1, respectively. The performance of our LFIA for CE2 and E7 detection was benchmarked against rapid ELISA (Fig. 4c). Our calculations yielded sensitivity of 94.7%, specificity of 90.5%, PPV of 90.0%, NPV of 95.0%, and accuracy of 92.5% (Fig. 4c). These findings suggest that our assay is highly sensitive and effective at correctly identifying TPs. The assay demonstrates better performance in identifying TNs than TPs, as evidenced by the higher NPV compared to the PPV. This implies the assay is particularly reliable for confirming the absence of anti-HPV16 antibodies, making it a valuable tool in screening applications where ruling out past/current infection is critical. The high sensitivity also supports its use in initial screenings to ensure few cases are missed.

We aimed to investigate the association between HPV16 infection and head and neck cancer. The LFIA test outcomes were compared to the actual patient cancer status to quantify the percentage of cancer patients and healthy individuals who tested positive or negative for anti-HPV16 antibodies (Fig. 4d). The results revealed that 66.7% of head and neck cancer patients and 20.0% of healthy individuals tested positive for anti-HPV16 antibodies. Among those with positive and negative LFIA test results, 90.9% and 55.6% were head and neck cancer cases, respectively. These findings suggest a moderate-to-high prevalence of HPV16 infection among head and neck cancer patients; however, they indicate that a significant percentage of head and neck cancer cases are not HPV16-driven. Furthermore, head and neck cancer does not necessarily imply HPV16 infection, nor does HPV16 infection guarantee the development of head and neck cancer.

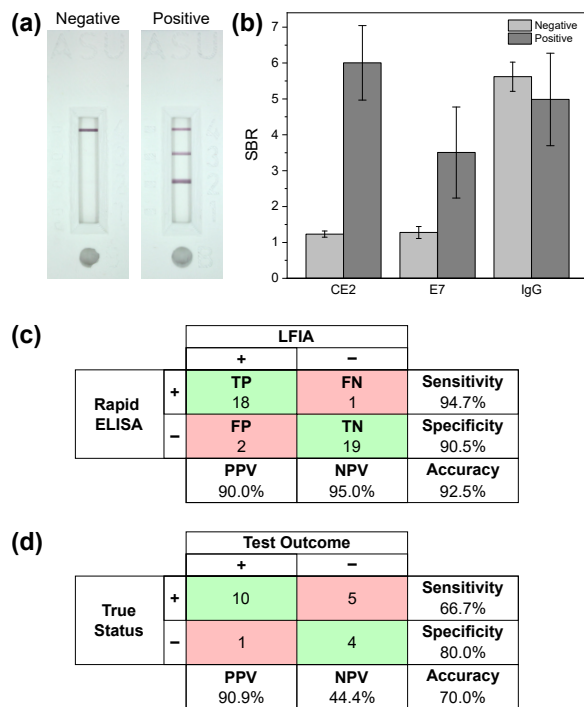


Fig. 4. (a) Images of negative and positive test results acquired with our colorimetric instrument. (b) Mean signal intensities for all negative and positive test results. (c) Confusion matrix benchmarking LFIA performance for CE2 and E7 detection against rapid ELISA. (d) LFIA test outcomes compared to true patient cancer status.

#### IV. CONCLUSION

In this study, we developed and validated a low-cost, open-source POC colorimetric detection platform targeting anti-HPV16 antibodies. Our system demonstrated adequate analytical sensitivity with a LOD at 46 ng/mL and robust clinical performance, achieving 94.7% sensitivity, 90.5% specificity and 92.5% overall accuracy. We determined significant prevalence of anti-HPV16 antibodies among head and neck cancer patients. The ability to detect low levels of anti-HPV16 CE2 and E7 antibodies with high clinical sensitivity highlights the efficacy of the proposed system

for ruling out healthy individuals and identifying those who require further diagnostic testing. The use of affordable, accessible hardware and software further enhances the potential for implementation in resource-constrained settings, where the burden of HPV is most significant and early detection is critical for effective intervention.

#### REFERENCES

- [1] K. P. Braaten and M. R. Laufer, "Human Papillomavirus (HPV), HPV-Related Disease, and the HPV Vaccine," *Reviews in Obstetrics & Gynecology*, vol. 1, no. 1, pp. 2–10, 2008.
- [2] K. Kobayashi, K. Hisamatsu, N. Suzui, A. Hara, H. Tomita, and T. Miyazaki, "A Review of HPV-Related Head and Neck Cancer," *Journal of Clinical Medicine*, vol. 7, p. 241, Aug. 2018.
- [3] V. D. Tsu, D. S. LaMontagne, P. Atuhebe, P. N. Bloem, and C. Ndiaye, "National implementation of HPV vaccination programs in low-resource countries: Lessons, challenges, and future prospects," *Preventive Medicine*, vol. 144, p. 106335, Mar. 2021.
- [4] R. Klaes, S. M. Woerner, R. Ridder, N. Wentzensen, M. Duerst, A. Schneider, B. Lotz, P. Melsheimer, and M. v. K. Doeberitz, "Detection of High-Risk Cervical Intraepithelial Neoplasia and Cervical Cancer by Amplification of Transcripts Derived from Integrated Papillomavirus Oncogenes1," *Cancer Research*, vol. 59, pp. 6132–6136, Dec. 1999.
- [5] P. Shende, B. Prabhakar, and A. Patil, "Color changing sensors: A multimodal system for integrated screening," *TrAC Trends in Analytical Chemistry*, vol. 121, p. 115687, Dec. 2019.
- [6] B. V. Vu, R. Lei, C. Mohan, K. Kourentzi, and R. C. Willson, "Flash Characterization of Smartphones Used in Point-of-Care Diagnostics," *Biosensors*, vol. 12, p. 1060, Nov. 2022.
- [7] Daniel. MacDougall, W. B. Crummett, and . Et Al., "Guidelines for data acquisition and data quality evaluation in environmental chemistry," *Analytical Chemistry*, vol. 52, pp. 2242–2249, Dec. 1980.
- [8] P. Di Bonito, F. Grasso, S. Mochi, L. Accardi, M. G. Donà, M. Branca, S. Costa, L. Mariani, A. Agarossi, M. Ciotti, K. Syrjänen, and C. Giorgi, "Serum antibody response to Human papillomavirus (HPV) infections detected by a novel ELISA technique based on denatured recombinant HPV16 L1, L2, E4, E6 and E7 proteins," *Infectious Agents and Cancer*, vol. 1, p. 6, Nov. 2006.
- [9] T. Little, "Method Validation Essentials, Limit of Blank, Limit of Detection, and Limit of Quantitation," *BioPharm International*, vol. 28, Mar. 2015.
- [10] J. Thode, "How to determine the LOD using the calibration curve?," *Lösungsfabrik*, June 2019.
- [11] C. Tong and M. Vendettuoli, "Parameterizations of the four-parameter logistic curve in software for estimating relative potency," *U.S. Department of Agriculture*, Mar. 2017.
- [12] H. Inan, S. Wang, F. Inci, M. Baday, R. Zangar, S. Kesiraju, K. S. Anderson, B. T. Cunningham, and U. Demirci, "Isolation, Detection, and Quantification of Cancer Biomarkers in HPV-Associated Malignancies," *Scientific Reports*, vol. 7, p. 3322, June 2017.
- [13] S. Parra, E. Carranza, J. Coole, B. Hunt, C. Smith, P. Keahey, M. Maza, K. Schmeler, and R. Richards-Kortum, "Development of Low-Cost Point-of-Care Technologies for Cervical Cancer Prevention Based on a Single-Board Computer," *IEEE Journal of Translational Engineering in Health and Medicine*, vol. 8, pp. 1–10, 2020.
- [14] B. Ujj, "Diagnostic Sensitivity and Specificity for Clinical Laboratory Testing," *Centers for Disease Control and Prevention*.
- [15] R. Parikh, A. Mathai, S. Parikh, G. Chandra Sekhar, and R. Thomas, "Understanding and using sensitivity, specificity and predictive values," *Indian Journal of Ophthalmology*, vol. 56, no. 1, p. 45, 2008.
- [16] A.-M. Šimundić, "Measures of Diagnostic Accuracy: Basic Definitions," *EJIFCC*, vol. 19, pp. 203–211, Jan. 2009.
- [17] H. B. Wong and G. H. Lim, "Measures of Diagnostic Accuracy: Sensitivity, Specificity, PPV and NPV," *Proceedings of Singapore Healthcare*, vol. 20, pp. 316–318, Dec. 2011.
- [18] J. Shreffler and M. R. Huecker, "Diagnostic Testing Accuracy: Sensitivity, Specificity, Predictive Values and Likelihood Ratios," *Europe PubMed Central*, Mar. 2023.
- [19] P. Eusebi, "Diagnostic Accuracy Measures," *Cerebrovascular Diseases*, vol. 36, no. 4, pp. 267–272, 2013.